Natural Resources for Human Health
eISSN: 2583-1194

Original Research

Received 18 May 2026
Revised 25 June 2026
Accepted 10 July 2026

Natural Resources for Human Health 2026, Vol. 6 (12s): 811–822

KEYWORDS:
Peripheral arterial disease, High fasting plasma glucose, Global Burden of Disease, Decomposition analysis, Forecasting, Socio-demographic Index

Global and Super-Regional Burden of Lower-Extremity Peripheral Arterial Disease Attributable to High Fasting Plasma Glucose, 1990–2023, with Projections to 2050: An Analysis of the Global Burden of Disease Study 2023

Mathhar Aldaoud MD[1*], Ricardo A Rodriguez Mejía MD[2], Kais Adli Albalbissi MD[3], Sarah Bassam Khirfan MD[4], Yazan Ayman Hammad MD[5], Yazan Michael Madaeen[6]

[1]School of medicine, University of Jordan Amman, Jordan
[2]Methodist university Cape Fear Valley school of medicine, Fayetteville, NC, USA, raqs2331@gmail.com
[3]School of medicine, University of Jordan Amman, Jordan. K.albalbissi@ju.edu.jo
[4]School of medicine, University of Jordan Amman, Jordan. Sarah.khirfan@yahoo.com
[5]School of medicine, University of Jordan Amman, Jordan. yazan.a.m.hammad@gmail.com
[6]yazanmadaeen358@gmail.com, School of medicine, University of Jordan Amman, Jordan
*Corresponding Author E-mail: M.Aldaoud@Ju.edu.jo

ABSTRACT:

Aims: To estimate, from the Global Burden of Disease Study 2023 (GBD 2023), how much lower-extremity peripheral arterial disease (LEAD) mortality and disability is due to high fasting plasma glucose (HFPG), 1990–2023; to separate drivers of the change in deaths; and to forecast mortality to 2050.

Methods: HFPG-attributable deaths, DALYs and age-standardised rates (ASMR, ASDR) were obtained globally, for five Socio-demographic Index (SDI) quintiles and seven GBD super-regions, by sex and age. Trends were expressed as estimated annual percentage change (EAPC); Das Gupta decomposition apportioned the change in deaths to population growth, ageing and rate change; five statistical, machine-learning and deep-learning models, compared on a 2019–2023 hold-out, projected global ASMR to 2050.

Results: Global ASMR and ASDR declined (EAPC −0.96% and −0.30% per year) while deaths rose by 12 132; population growth (+11 595) and ageing (+4 048) outweighed epidemiological improvement (−4 132). Rates increased in the three lowest SDI quintiles and in North Africa and the Middle East (4.78%/year), South Asia (2.91%) and Sub-Saharan Africa (2.52%), climbed sharply with age and were higher in men; by 2050 global ASMR is expected to be about 0.19 per 100 000 (range 0.15–0.20).

Conclusions: Rates are improving worldwide, yet deaths keep rising because populations are larger and older, and rates are worsening in lower-SDI settings, where glycaemic control and limb care most need expanding.

1. INTRODUCTION

When atherosclerosis narrows or blocks the arteries that supply the legs, the result is lower-extremity peripheral arterial disease (LEAD), a condition in which limb perfusion falls progressively [1, 2]. Its consequences range from walking impairment and loss of independence to chronic limb-threatening ischaemia and amputation [3], and its presence identifies people at high risk of coronary events, stroke and premature death [4]. Pooled prevalence studies put the number of affected people at roughly 202 million in 2010 and 237 million in 2015, more than two-thirds of whom lived in low- and middle-income countries [5, 6]; the GBD, which applies a stricter case definition, counted over 113 million prevalent cases in 2019 [7]. As populations age, these numbers are projected to keep growing [7, 8], so LEAD will matter more for public health even where rates within each age group improve. Among metabolic risk factors, high fasting plasma glucose (HFPG) ranks with the largest contributors to cardiovascular health loss worldwide [9, 10]. Exposure is growing as diabetes spreads and populations age [11, 12]: the IDF Diabetes Atlas expects 783 million adults to have diabetes by 2045 [12]. Chronic hyperglycaemia damages the vasculature through several linked pathways: endothelial dysfunction, oxidative stress and persistent inflammation in the arterial wall, which together promote atherogenesis and plaque progression [13, 14]. These changes reduce distal blood flow and predispose the lower-limb arteries to occlusion [15]. Having diabetes approximately doubles the chance of developing LEAD; in the UK Prospective Diabetes Study, every percentage-point increase in HbA1c carried a 28% excess risk of peripheral vascular disease after adjustment for other factors [16, 17]. Hyperglycaemia also shifts disease toward the distal, heavily calcified arteries, where revascularisation is more difficult [18]. People with elevated fasting glucose therefore develop LEAD more often and experience worse limb outcomes, including chronic limb-threatening ischaemia, foot ulceration and amputation [7, 19, 20]. In a 2024 systematic review of 80 studies, LEAD in people with type 2 diabetes was associated with frequent limb events, cardiovascular events and substantial health-care expenditure [21]. The biological and epidemiological link between HFPG and LEAD is therefore well established. Several groups have used Global Burden of Disease (GBD) estimates to map LEAD and the risk factors behind it [7, 22–24], and the share of stroke, cancer and colorectal cancer burden due to HFPG has been quantified in the same way [25–28]. In both GBD 2019 and GBD 2021, no modifiable risk factor accounted for more LEAD deaths and disability-adjusted life-years (DALYs) than HFPG, and its share grew over time [7, 29–31], and the burden was concentrated in older adults, in men for mortality, and in high-SDI settings for absolute counts, with the fastest relative increases in lower-SDI regions [29–32]. A recent GBD 2021 analysis specific to HFPG-attributable LEAD reported 25 640 deaths and 562 161 DALYs in 2021 and rising age-standardised rates in low- and middle-income settings [30]. Several gaps remain. First, all published estimates of HFPG-attributable LEAD rest on GBD 2019 or GBD 2021 [7, 29, 30]; GBD 2023, released in October 2025, updated the cause and risk models and extended the series to 2023 [9], and no analysis of HFPG-attributable LEAD based on it has yet appeared to the best of our knowledge. Second, earlier studies reported how attributable deaths changed over time but did not apportion that change between a larger population, an older population and altered age-specific rates [8, 33]. Such decomposition has been informative for all-cause mortality and for other HFPG-related outcomes [27, 28, 34], but has not been applied to LEAD, leaving open whether the rising counts reflect deteriorating rates or demography alone. Third, forecasts of HFPG-attributable LEAD burden are scarce; existing projections address LEAD as a whole [8, 31] or cardiovascular disease more broadly [35], and rely on a single model family. Fourth, no study has combined updated burden estimates, trend assessment, decomposition and multi-model forecasting for this risk–outcome pair within a single analytical framework. We therefore set out to measure, with GBD 2023 estimates, how much LEAD mortality and disability was due to HFPG between 1990 and 2023 for the world, for Socio-demographic Index (SDI) quintiles and for the seven GBD super-regions. Four indicators are reported—attributable deaths, DALYs, age-standardised mortality rates (ASMRs) and age-standardised DALY rates (ASDRs)—together with estimated annual percentage change (EAPC), age- and sex-specific patterns, a decomposition of the change in deaths into demographic and rate components, and a projection of global ASMR to 2050 that compares statistical, machine-learning and deep-learning models.

2. MATERIALS AND METHODS

2.1. Study design and data source

We re-analysed published estimates from the 2023 round of the Global Burden of Diseases, Injuries, and Risk Factors Study (GBD 2023), which is coordinated by the Institute for Health Metrics and Evaluation (IHME) [9, 36], retrieving them through the GBD Results Tool [37]. The GBD combines death registration, verbal autopsies, disease surveillance, censuses, household surveys and registries in one modelling system, and reconciles incidence, prevalence and mortality with each other through the Bayesian meta-regression package DisMod-MR 2.1 [9]. Every estimate carries a 95% uncertainty interval (UI) taken from the

2.5th and 97.5th percentiles of 1 000 posterior draws. No individual-level data were accessed—only aggregated public estimates—so no ethics committee review or consent was needed. The manuscript is written to conform with the GATHER reporting guidance for health estimates [38].

2.2. Case and exposure definitions

LEAD, the outcome, is identified in the GBD by an ankle–brachial index ≤0.90 and, for deaths, by ICD-10 codes I70.2–I70.7 and I73.9 [7, 9]. HFPG, the exposure, is treated by the GBD as a continuous variable; excess risk is counted above a theoretical minimum risk exposure level (TMREL) set at 4.8–5.4 mmol/L [10, 39]. HFPG therefore captures the full glycaemic continuum, including impaired fasting glucose below the diagnostic threshold for diabetes, rather than diagnosed diabetes alone; the WHO and ADA fasting-glucose thresholds for diabetes both lie well above the TMREL [40]. The share of LEAD deaths and DALYs due to HFPG comes from the comparative risk assessment in the GBD: a population attributable fraction (PAF) is computed separately by location, year, age and sex and multiplied by the matching LEAD totals [10].

2.3. Geographic and temporal scope, and indicators

The GBD sorts locations by development level with the SDI, a 0–1 index built from lagged per-capita income, average schooling and fertility below age 25 [41]. We analysed the world as a whole, each of the five SDI quintiles (low to high) and the seven GBD super-regions (Central Europe, Eastern Europe and Central Asia; high-income; Latin America and Caribbean; North Africa and Middle East; South Asia; Southeast Asia, East Asia and Oceania; Sub-Saharan Africa) over 1990–2023, projecting forward to 2050. Results are broken down by sex and by ten five-year age bands from 50–54 to 95+ years, the ages at which nearly all HFPG-attributable LEAD deaths occur. Four indicators were examined: attributable deaths and DALYs (counts), the ASMR and ASDR per 100 000, and the PAF. For a continuous exposure the PAF is

$$PAF = \frac{\int_x RR_x P_x dx - \int_x RR_x P_x^* dx}{\int_x RR_x P_x dx} \quad (1)$$

in which RRx denotes the relative risk at exposure x, Px the exposure distribution actually observed and P*x the counterfactual distribution if everyone were at the TMREL.

2.4. Age standardisation and trend estimation

Age-standardised rates (ASRs) were computed directly against the GBD world standard population [9],

$$ASR = \frac{\sum_{i=1}^{A} r_i w_i}{\sum_{i=1}^{A} w_i} \times 10^5 \quad (2)$$

where ri and wi are, respectively, the rate and the standard-population weight in age group i. Long-run trends were expressed as the EAPC. Fitting ln(ASRt) = α + βt + εt to the annual series gives [42]

$$EAPC = 100 \times \left(e^{\beta} - 1\right), \quad CI = 100 \times \left(e^{\beta \pm z_{1-\alpha/2} SE(\beta)} - 1\right) \quad (3)$$

We classed a trend as rising if the EAPC and the lower limit of its 95% confidence interval (CI) both exceeded zero, as falling if the EAPC and its upper limit were both negative, and as stable in all other cases.

2.5. Decomposition analysis

Following Das Gupta [43], the difference in attributable deaths between 1990 and 2023 was split into three parts—growth in population size, shifts in its age structure, and changes in age-specific rates (the epidemiological component),

$$\Delta B = \Delta B_{growth} + \Delta B_{ageing} + \Delta B_{epi} \quad (4)$$

each part being calculated with the other two factors fixed at the mean of their 1990 and 2023 values. Added together, the three parts reproduce the modelled change, which closely tracks the observed one.

2.6. Comparative forecasting framework

Five models from three families were used to project global ASMR to 2050: two statistical models, ARIMA and exponential smoothing (ETS), whose orders were chosen by information criteria [44, 45]; the gradient-boosted tree ensemble XGBoost [46]; and two neural networks, the long short-term memory (LSTM) recurrent network [47] and N-BEATS, a basis-expansion architecture for time series [48]. The observed series is short (34 annual points) and dominated by a smooth secular decline, a

setting in which flexible models are prone to over-fitting and in which GBD forecasting work has likewise relied on trend-anchored approaches [49], so all models were cast in a shared trend-component framework rather than being allowed to re-extrapolate the trend independently. Each series was expressed as a deterministic log-linear trend plus a stationary residual,

$$ln(rate_t) = a + bt + e_t \quad (5)$$

and each model forecast only the residual et, which was then recombined with the trend and exponentiated. Models were trained on 1990–2018 and validated on the 2019–2023 hold-out. Forecast error on the hold-out was measured three ways—RMSE, MAE and MAPE:

$$RMSE = \sqrt{\frac{1}{n}\sum_t (y_t - \hat{y}_t)^2}, \quad MAE = \frac{1}{n}\sum_t |y_t - \hat{y}_t| \quad (6)$$

$$MAPE = \frac{100}{n}\sum_t \left|\frac{y_t - \hat{y}_t}{y_t}\right| \quad (7)$$

The model with the lowest hold-out error was adopted for the headline projection. Because all five models share the same deterministic trend, the headline projection is in effect a trend extrapolation, and its sensitivity to the estimation window was assessed by refitting the trend on the full 1990–2023 period and on the most recent decade; the projection is therefore reported as a central estimate with a plausible range. A 95% prediction interval was derived from the parameter and residual uncertainty of the fitted log-linear trend. The machine-learning and deep-learning models served as sensitivity and robustness checks: agreement with the statistical models indicates that no material non-linear signal remains in the residual, and they were not used as headline forecasts.

2.7. Software

All analyses were performed in Python 3.11. ARIMA and ETS were fitted with *statsmodels*; XGBoost with *xgboost*; LSTM and N-BEATS with *PyTorch*; trend, decomposition and numerical work used *NumPy*, *pandas*, *SciPy* and *scikit-learn*; figures were produced with *Matplotlib* using the perceptually uniform viridis colour map.

3. RESULTS

3.1. Global trends, 1990–2023

Between 1990 and 2023 the world ASMR and ASDR for HFPG-attributable LEAD both moved downward in men and in women (Fig. 1): the ASMR by −0.96% a year (95% CI −1.11 to −0.82) and the ASDR by −0.30% a year (95% CI −0.38 to −0.21) (Table 1). At every point in the series men had higher rates than women, with the 95% UIs of the two sexes largely non-overlapping. Mortality and total health loss tracked each other closely, as the parallel panels of Fig. 1 show. Even so, 12 132 more deaths were attributable to HFPG in 2023 than in 1990 (Table 2).

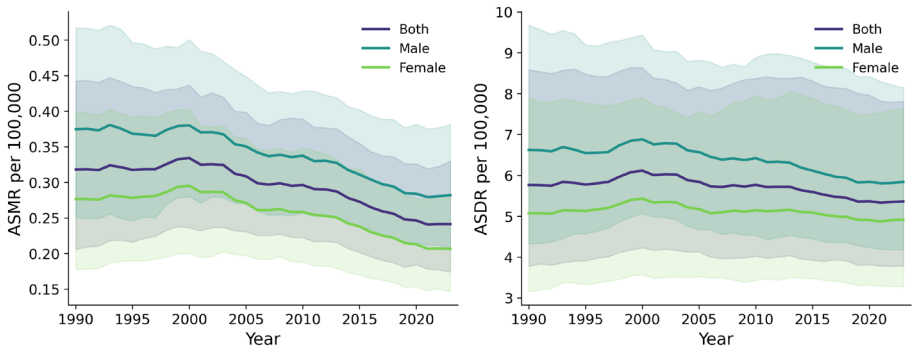

Fig. 1 Worldwide trends in HFPG-attributable LEAD by sex, 1990–2023. Left: ASMR per 100 000; right: ASDR per 100 000. Lines are point estimates (both sexes, men, women); bands are 95% UIs. Abbreviations as in text

3.2. Age- and sex-specific mortality, 2023

The age gradient was steep (Supplementary Fig. S1): mortality was close to zero before 65 years, climbed from 65–69 years onward and peaked at 95 years and above. Up to 90–94 years men died at higher rates than women; only in the 95+ band did

women overtake men. This pattern is consistent with the age-related accumulation of atherosclerotic disease and with known sex differences in limb outcomes, with the reversal in the oldest group likely reflecting the survival of women to very old age.

3.3. Trends by SDI quintile and super-region

EAPCs for every geographic unit are listed in Table 1. Behind the roughly 1% annual global decline lay sharply different regional trends. ASMR increased in the low (2.84% a year), low-middle (2.22%) and middle (2.32%) SDI quintiles, held steady in the high-middle quintile (−0.04%, 95% CI −0.12 to 0.04) and decreased in the high quintile (−0.97%). The steepest super-regional rise was in North Africa and the Middle East (4.78% a year), then South Asia (2.91%) and Sub-Saharan Africa (2.52%), with a small increase in Southeast Asia, East Asia and Oceania (0.28%); Latin America and Caribbean was flat, while the high-income super-region (−0.48%) and Central Europe, Eastern Europe and Central Asia (−0.70%) improved. ASMR and ASDR trends pointed the same way everywhere except in the high-middle SDI quintile and the high-income super-region, where the DALY rate was flat or edging up while the mortality rate was flat or falling.

Figure 2 plots the seven super-regional ASMR series and ranks them by EAPC. Throughout the period the highest rates were in Central Europe, Eastern Europe and Central Asia and in the high-income super-region, yet both fell; Sub-Saharan Africa, by contrast, more than doubled from about 0.15 to about 0.34 per 100 000 and passed Latin America and Caribbean after 2005. North Africa and the Middle East and South Asia started from low levels and roughly tripled and doubled, respectively. The divergence between the three super-regions with positive EAPC and the two with negative EAPC identifies where HFPG-attributable LEAD is an expanding rather than a receding public-health problem.

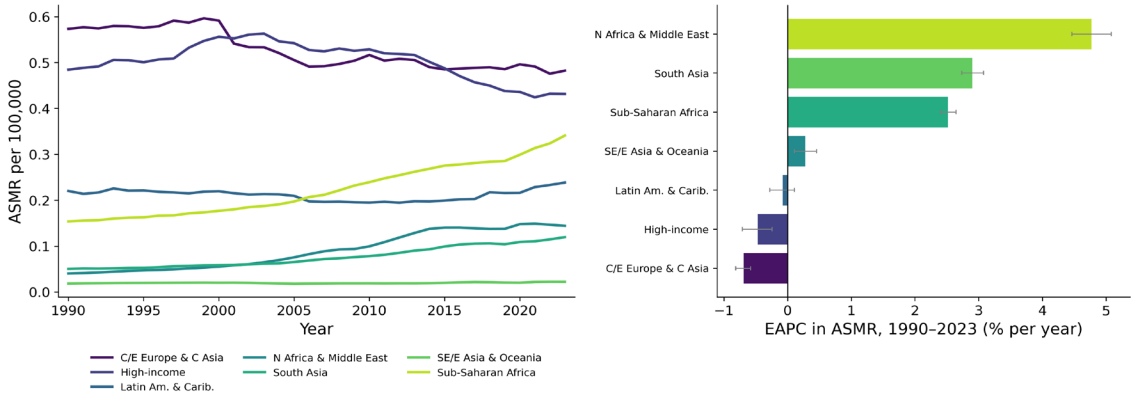

Fig. 2 HFPG-attributable LEAD mortality across the seven GBD super-regions, 1990–2023. Left: ASMR per 100 000 over time. Right: super-regions ordered by EAPC in ASMR (bars) with 95% CIs (whiskers). Abbreviations as in text

Table 1 EAPC in ASMR and ASDR of HFPG-attributable LEAD by SDI quintile and super-region, 1990–2023

Location	EAPC in ASMR, % (95% CI)	EAPC in ASDR, % (95% CI)
Global	−0.96 (−1.11 to −0.82)	−0.30 (−0.38 to −0.21)
Low SDI	2.84 (2.69 to 2.99)	2.13 (2.01 to 2.24)
Low-middle SDI	2.22 (2.03 to 2.41)	1.18 (1.07 to 1.28)
Middle SDI	2.32 (2.22 to 2.41)	1.08 (1.05 to 1.11)
High-middle SDI	−0.04 (−0.12 to 0.04)	0.57 (0.53 to 0.62)
High SDI	−0.97 (−1.17 to −0.78)	−0.47 (−0.61 to −0.33)
Central Europe, Eastern Europe and Central Asia	−0.70 (−0.81 to −0.58)	−0.55 (−0.65 to −0.44)

Location	EAPC in ASMR, % (95% CI)	EAPC in ASDR, % (95% CI)
High-income	−0.48 (−0.71 to −0.24)	−0.06 (−0.24 to 0.12)
Latin America and Caribbean	−0.08 (−0.28 to 0.11)	0.14 (−0.01 to 0.29)
North Africa and Middle East	4.78 (4.47 to 5.08)	2.98 (2.78 to 3.19)
South Asia	2.91 (2.73 to 3.08)	1.43 (1.34 to 1.52)
Southeast Asia, East Asia and Oceania	0.28 (0.11 to 0.45)	0.48 (0.41 to 0.55)
Sub-Saharan Africa	2.52 (2.40 to 2.65)	2.33 (2.22 to 2.45)

Entries are annual percentage changes from a log-linear fit of each rate against year, with 95% CIs. Abbreviations as in text

3.4. Decomposition of the change in attributable deaths

The decomposition is given in Table 2. Worldwide, a larger population contributed 11 595 additional deaths and an older population 4 048, whereas falling age-specific rates subtracted 4 132, leaving a net gain of 12 132. Development level changed the balance. In the high SDI quintile and the high-income super-region a sizeable favourable rate component (−3 656 and −1 296) absorbed part of the demographic push. In the three lowest SDI quintiles and in North Africa and the Middle East, South Asia and Sub-Saharan Africa the rate component was itself positive (+185 to +527), adding to rather than offsetting growth and ageing. Ageing alone explained about half or more of the increase in the high-income super-region (+3 113) and in Central Europe, Eastern Europe and Central Asia (+728).

Table 2 Contributions of population growth, ageing and rate change to the 1990–2023 change in HFPG-attributable LEAD deaths

Location	Population growth	Population ageing	Epidemiological change	Observed change
Global	11 595	4 048	−4 132	12 132
Low SDI	513	79	514	1 083
Low-middle SDI	302	88	243	612
Middle SDI	235	36	185	444
High-middle SDI	964	344	57	1 387
High SDI	7 937	3 836	−3 656	8 587
Central Europe, Eastern Europe and Central Asia	740	728	−485	997
High-income	4 790	3 113	−1 296	6 826
Latin America and Caribbean	873	161	75	1 099
North Africa and Middle East	207	27	222	443
South Asia	550	169	480	1 146
Southeast Asia, East Asia and Oceania	313	114	66	482

Location	Population growth	Population ageing	Epidemiological change	Observed change
Sub-Saharan Africa	581	37	527	1 139

Entries are numbers of deaths. The three components add to the modelled change; the small gap to the observed change is the interaction term. Abbreviations as in text

3.5. Forecasting accuracy and projections to 2050

On the 2019–2023 hold-out, ETS had the lowest error (RMSE 0.0068, MAPE 2.71%), followed by ARIMA (RMSE 0.0082, MAPE 3.31%) (Supplementary Table S1). XGBoost, LSTM and N-BEATS produced near-identical errors (RMSE 0.0196, MAPE 7.62–7.65%), indicating that, once the common trend was removed, these models recovered no additional forecastable structure from the residual. ETS was therefore adopted for the headline projection.

All five models projected a continued decline in global ASMR through 2050 (Fig. 3, Supplementary Table S2). The projections converged because the models share a deterministic trend; their agreement should therefore be read as confirmation that no material non-linear signal was present, not as independent corroboration. The central ETS projection was 0.225 per 100 000 in 2030 and 0.186 in 2050 (95% prediction interval 0.172–0.216). The projection was sensitive to the estimation window: extrapolating the trend fitted to the full 1990–2023 period gave approximately 0.20 per 100 000 in 2050, whereas extrapolating the most recent decade gave approximately 0.15, defining a plausible range of 0.15–0.20 per 100 000. Read alongside the decomposition, a declining rate does not rule out a further increase in deaths: growing and ageing populations can outpace it.

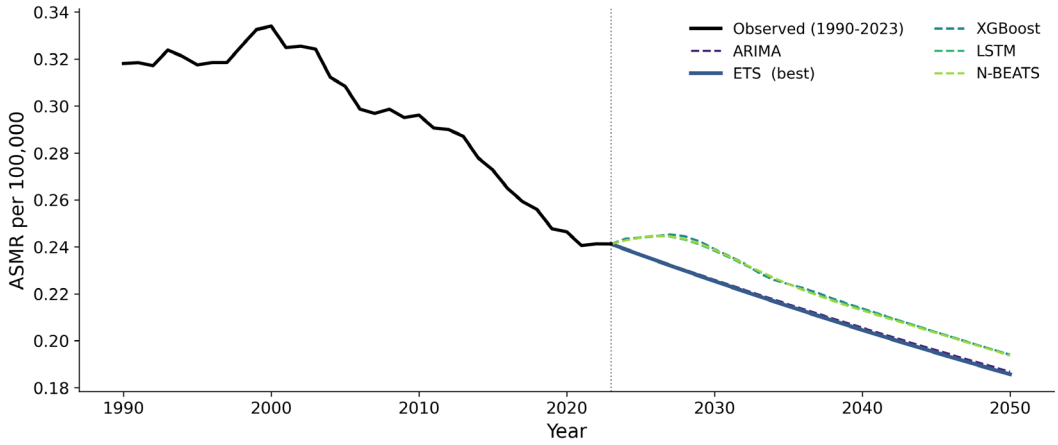

Fig. 3 Global ASMR of HFPG-attributable LEAD: observed series (1990–2023) and projections to 2050 from ARIMA, ETS, XGBoost, LSTM and N-BEATS fitted within the common trend-component framework. Model abbreviations as in Section 2.6

4. DISCUSSION

Drawing on GBD 2023, we have traced HFPG-attributable LEAD from 1990 to 2023 and projected it to 2050. Four points emerge. First, global age-standardised mortality and DALY rates have been falling since 1990 and were still falling in 2023. Second, deaths have nonetheless risen, because the demographic push from bigger and older populations was only about a quarter offset by the improvement in rates. Third, the global mean hides deterioration in the three lowest SDI quintiles and in North Africa and the Middle East, South Asia and Sub-Saharan Africa. Fourth, the burden falls mainly on older adults and, below 95 years, on men. Comparative forecasting indicates that the global age-standardised rate will keep falling to 2050, with the caveat that absolute counts may keep rising.

4.1. Comparison with previous studies

Our global trends point the same way as earlier GBD analyses. Kim et al. found age-standardised PAD prevalence falling between 1990 and 2019 while case numbers rose [7], and Zhang et al. found that ASMR and ASDR for LEAD fell over 1990–2021 while deaths and DALYs increased [31]. For the HFPG-attributable fraction specifically, Qu et al. estimated 25 640 deaths

and 562 161 DALYs in 2021 with global ASMR and ASDR of 0.32 and 6.73 per 100 000 [30]; our 2023 values are of the same order, and the differences reflect both the additional two years and the model revisions introduced in GBD 2023 [9]. Our results extend these studies by confirming that the favourable trend persisted through 2023 and by showing, through decomposition, that the increase in counts is a demographic rather than an epidemiological phenomenon at the global level. The same demographic dominance has been reported for all-cause mortality and for HFPG-attributable ischaemic stroke and colorectal cancer [27, 28, 34], which suggests that the pattern reflects the global epidemiological transition rather than anything specific to LEAD.

Part of the decline in rates is plausibly explained by better control of cardiovascular risk factors: improved diabetes management, wider use of lipid-lowering and antihypertensive therapy, smoking cessation and expanded evidence-based vascular care [1, 2]. Improvements in glycaemic control and access to glucose-lowering agents may have reduced the vascular complications of hyperglycaemia in particular [11]. The decomposition shows, however, that these gains have not been large enough to offset demographic change, even in high-SDI settings where the epidemiological component was most favourable.

4.2. Why hyperglycaemia matters for the lower limb

The attributable fraction that drives these estimates rests on a causal relationship with a clear biological basis. Sustained hyperglycaemia drives glycation of proteins and accumulation of advanced glycation end-products, switches on protein kinase C together with the polyol and hexosamine pathways, and raises mitochondrial superoxide output; these converge on an endothelium that releases less nitric oxide and an arterial wall that is oxidatively stressed, inflamed and prone to thrombosis [13, 14, 18]. In type 2 diabetes, indices of oxidative damage rise with poorer glycaemic control and are higher in those who already have vascular complications [50]. In the lower limb these processes favour diffuse, distal (infrapopliteal) atherosclerosis and medial arterial calcification, which reduce the options for revascularisation and, together with neuropathy and impaired wound healing, account for the much higher frequency of foot ulcers and amputations when LEAD coexists with diabetes [15, 18–20]. Because the GBD relative risks for HFPG apply across the glycaemic continuum, part of the attributable burden arises in people with impaired fasting glucose who have not been diagnosed with diabetes, a group in which LEAD is rarely sought.

4.3. Regional and socio-demographic heterogeneity

Regionally, our findings resemble those for LEAD overall [7, 31, 32] and for other conditions attributable to HFPG [10]: improvement where SDI and income are high, deterioration where SDI is lower and in the three super-regions in which rapid demographic transition coincides with a steep rise in diabetes. Criqui et al. attributed such variation to differences in access to health care, control of cardiovascular risk factors and disease awareness [1]. Urbanisation, growing obesity and diabetes, changing diets, sedentary living and continued smoking have rapidly reshaped metabolic risk in many low- and middle-income settings [11]. Care systems have not kept pace: preventive services are thin, diabetes is often detected late—the IDF estimates that nearly one in two adults with diabetes is undiagnosed, most of them in low- and middle-income countries [51]—LEAD is seldom sought, glycaemia is poorly controlled and specialist vascular services are scarce. The positive epidemiological component in these settings (Table 2) indicates that age-specific mortality is still increasing there, in contrast to the high-income experience. The GBD 2023 estimates thus support region-specific prevention strategies and a redistribution of vascular and diabetes care resources toward settings where the burden is growing fastest.

4.4. Age and sex patterns

The steep age gradient agrees with previous descriptions of LEAD epidemiology [2, 29, 31, 32] and with the age-related progression of endothelial dysfunction, arterial stiffening, chronic inflammation and atherosclerosis [13, 15]. Men had higher mortality than women in every age group below 95 years, consistent with earlier reports [1, 2, 31], and plausibly reflecting differences in smoking history, cumulative exposure to atherosclerotic risk factors, hormonal protection and sex-specific disease progression. The crossover in the 95+ group, where the rate in women exceeded that in men, has also been observed for all-cause LEAD burden among the very old [29, 32] and is likely a survival effect. These patterns argue for targeted screening and prevention among older adults, and particularly among older men with diabetes or elevated fasting glucose.

4.5. Clinical and policy implications

Three implications follow. First, guidelines already call for an ankle–brachial index whenever a person with diabetes has symptoms or signs suggestive of LEAD, and for a foot examination at least yearly in everyone with diabetes [52, 53]; our age–sex results indicate that yield will be highest in men aged 65 years and above and in the very old of both sexes, and that screening

should not be confined to those with a diabetes diagnosis when fasting glucose is known to be elevated. Second, glycaemic control remains the modifiable lever specific to the attributable fraction reported here; hyperglycaemia was an independent, modifiable predictor of peripheral vascular disease in the UK Prospective Diabetes Study [16], and the guideline-recommended combination of glucose lowering with lipid, blood-pressure and antiplatelet therapy addresses the wider atherosclerotic risk [52, 53]. Third, at the health-system level the decomposition identifies where investment will matter most: in the three super-regions with a positive epidemiological component, the priority is earlier diagnosis of dysglycaemia—a recent meta-analysis found LEAD in close to one in three people with diabetes in sub-Saharan Africa [54]—together with basic vascular assessment in primary care; in high-income settings, where the epidemiological component is favourable, the task is to sustain risk-factor control in an ageing population. Diabetes-focused programmes that monitor limb outcomes, rather than glycaemia alone, would allow the projected fall in age-standardised rates to be tracked against the rising absolute counts.

4.6. Strengths and weaknesses of the study

This study draws on the newest GBD cycle, brings trend analysis, decomposition and forecasting to bear on one risk–outcome pair, and uses a forecasting design that limits over-interpretation of a short series by tying all models to one trend and scoring them on withheld years. It also has weaknesses. First, the GBD produces modelled rather than directly observed values, and how well they reflect reality depends on the data each country supplies; where vital registration is sparse, as in much of the low-SDI world, LEAD seldom appears as an underlying cause of death, and the resulting UIs are wide. Second, the attributable burden depends on the assumed relative risks and the TMREL for HFPG; changes to these inputs between GBD cycles limit direct comparison with GBD 2019- and GBD 2021-based estimates. Third, analyses were restricted to ages 50 years and above and to super-regions and SDI quintiles; country-level estimates were not examined, so within-region heterogeneity is not described. Fourth, the forecasting series contains only 34 annual points, and all models were constrained to a shared trend; the projections are therefore trend extrapolations with a sensitivity range rather than independent forecasts, and the deep-learning models add robustness rather than predictive gain in this setting. Bayesian age–period–cohort models used in related work [23, 31] would offer an alternative, but they depend on the same short series and share the same limitation. Fifth, the forecasts extend the present trend forward; they make no allowance for future shifts in diabetes prevalence, in treatment coverage or in how deaths are certified. Finally, the ecological design does not permit causal inference at the individual level.

4.7. CONCLUSIONS

In this GBD 2023 analysis, HFPG-attributable LEAD mortality and disability rates have declined worldwide since 1990, yet larger and older populations have pushed the number of deaths upward, and rates are moving the wrong way in the lower-SDI quintiles and in three super-regions. The global ASMR should keep falling to 2050, most plausibly to between 0.15 and 0.20 per 100 000. The disparities by region, development level, age and sex point to a need for more equitable access to diabetes and vascular care and for prevention focused on older adults with elevated glucose. Validation against national and subnational data, and evaluation of how improved glycaemic control and earlier LEAD screening would alter the projected burden, are the next steps.

FUNDING

This research did not receive any specific grant from funding agencies in the public, commercial, or not-for-profit sectors.

DECLARATION OF COMPETING INTEREST

The authors declare that they have no known competing financial interests or personal relationships that could have appeared to influence the work reported in this paper.

REFERENCES

[1] Criqui MH, Matsushita K, Aboyans V, Hess CN, Hicks CW, Kwan TW, et al. Lower extremity peripheral artery disease: contemporary epidemiology, management gaps, and future directions: a scientific statement from the American Heart Association. Circulation. 2021;144(9):e171–91.

[2] Aday AW, Matsushita K. Epidemiology of peripheral artery disease and polyvascular disease. Circ Res. 2021;128(12):1818–32.

[3] Berchiolli R, Bertagna G, Adami D, Canovaro F, Torri L, Troisi N. Chronic limb-threatening ischemia and the need for revascularization. J Clin Med. 2023;12(7):2682.

[4] Minc SD, McGinigle KL. Peripheral artery disease: new concepts, treatments, and disparities. Annu Rev Med. 2026;77(1):45–58.

[5] Fowkes FGR, Rudan D, Rudan I, Aboyans V, Denenberg JO, McDermott MM, et al. Comparison of global estimates of prevalence and risk factors for peripheral artery disease in 2000 and 2010: a systematic review and analysis. Lancet. 2013;382(9901):1329–40.

[6] Song P, Rudan D, Zhu Y, Fowkes FJI, Rahimi K, Fowkes FGR, et al. Global, regional, and national prevalence and risk factors for peripheral artery disease in 2015: an updated systematic review and analysis. Lancet Glob Health. 2019;7(8):e1020–30.

[7] Kim MS, Hwang J, Yon DK, Lee SW, Jung SY, Park S, et al. Global burden of peripheral artery disease and its risk factors, 1990–2019: a systematic analysis for the Global Burden of Disease Study 2019. Lancet Glob Health. 2023;11(10):e1553–65.

[8] Deng L, Du C, Liu L, Wang Y, Gu H, Armstrong DG, et al. Forecasting the global burden of peripheral artery disease from 2021 to 2050: a population-based study. Research (Wash D C). 2025;8:0702.

[9] GBD 2023 Diseases, Injuries, and Risk Factors Collaborators. Burden of 375 diseases and injuries, risk-attributable burden of 88 risk factors, and healthy life expectancy in 204 countries and territories, including 660 subnational locations, 1990–2023: a systematic analysis for the Global Burden of Disease Study 2023. Lancet. 2025;406(10513):1873–922.

[10] GBD 2021 Risk Factors Collaborators. Global burden and strength of evidence for 88 risk factors in 204 countries and 811 subnational locations, 1990–2021: a systematic analysis for the Global Burden of Disease Study 2021. Lancet. 2024;403(10440):2162–203.

[11] Ong KL, Stafford LK, McLaughlin SA, Boyko EJ, Vollset SE, Smith AE, et al. Global, regional, and national burden of diabetes from 1990 to 2021, with projections of prevalence to 2050: a systematic analysis for the Global Burden of Disease Study 2021. Lancet. 2023;402(10397):203–34.

[12] Sun H, Saeedi P, Karuranga S, Pinkepank M, Ogurtsova K, Duncan BB, et al. IDF Diabetes Atlas: global, regional and country-level diabetes prevalence estimates for 2021 and projections for 2045. Diabetes Res Clin Pract. 2022;183:109119.

[13] Yang DR, Wang MY, Zhang CL, Wang Y. Endothelial dysfunction in vascular complications of diabetes: a comprehensive review of mechanisms and implications. Front Endocrinol. 2024;15:1359255.

[14] Binjawhar DN, Alhazmi AT, Bin Jawhar WN, MohammedSaeed W, Safi SZ. Hyperglycemia-induced oxidative stress and epigenetic regulation of ET-1 gene in endothelial cells. Front Genet. 2023;14:1167773.

[15] Takahara M. Diabetes mellitus and peripheral artery disease. Diabetol Int. 2025;16(1):7–12.

[16] Adler AI, Stevens RJ, Neil A, Stratton IM, Boulton AJM, Holman RR. UKPDS 59: hyperglycemia and other potentially modifiable risk factors for peripheral vascular disease in type 2 diabetes. Diabetes Care. 2002;25(5):894–9.

[17] Selvin E, Marinopoulos S, Berkenblit G, Rami T, Brancati FL, Powe NR, et al. Meta-analysis: glycosylated hemoglobin and cardiovascular disease in diabetes mellitus. Ann Intern Med. 2004;141(6):421–31.

[18] Beckman JA, Creager MA, Libby P. Diabetes and atherosclerosis: epidemiology, pathophysiology, and management. JAMA. 2002;287(19):2570–81.

[19] Armstrong DG, Boulton AJM, Bus SA. Diabetic foot ulcers and their recurrence. N Engl J Med. 2017;376(24):2367–75.

[20] Prompers L, Huijberts M, Apelqvist J, Jude E, Piaggesi A, Bakker K, et al. High prevalence of ischaemia, infection and serious comorbidity in patients with diabetic foot disease in Europe: baseline results from the Eurodiale study. Diabetologia. 2007;50(1):18–25.

[21] Verma S, Leiter LA, Mangla KK, Nielsen NF, Hansen Y, Bonaca MP. Epidemiology and burden of peripheral artery disease in people with type 2 diabetes: a systematic literature review. Diabetes Ther. 2024;15(9):1893–961.

[22] Vaduganathan M, Mensah GA, Turco JV, Fuster V, Roth GA. The global burden of cardiovascular diseases and risk: a compass for future health. J Am Coll Cardiol. 2022;80(25):2361–71.

[23] He Y, Zhou M, Tang J, Zheng Y, Chen J, Xing B, et al. Global, regional, and national burden of lower extremity peripheral arterial disease: a systematic analysis of prevalence, incidence, deaths, and DALYs from 1990 to 2021 with projections and dietary risk factors to 2036. J Health Popul Nutr. 2025;44:351.

[24] Liu W, Cui C. Global and national burden of peripheral arterial disease from 1990 to 2021: a systematic analysis of Global Burden of Disease Study 2021. Front Cardiovasc Med. 2025;12:1603810.

[25] Liu Y, Wang W, Huang X, Zhang X, Lin L, Qin JJ, et al. Global disease burden of stroke attributable to high fasting plasma glucose in 204 countries and territories from 1990 to 2019: an analysis of the Global Burden of Disease Study. J Diabetes. 2022;14. doi:10.1111/1753-0407.13299.

[26] Safiri S, Nejadghaderi SA, Karamzad N, Kaufman JS, Carson-Chahhoud K, Bragazzi NL, et al. Global, regional and national burden of cancers attributable to high fasting plasma glucose in 204 countries and territories, 1990–2019. Front Endocrinol. 2022;13:879890.

[27] Dong Y, Wang Y, Lan X, Zeng H. Epidemiological and demographic drivers of ischemic stroke attributed to high fasting plasma glucose from 1990 to 2021: findings from the 2021 Global Burden of Disease Study. Front Public Health. 2025;13:1511518.

[28] Gao N, Yang N, Huang J. Decomposition and forecasting of colorectal cancer burden attributable to high body mass index and high fasting plasma glucose, 1990–2021: a GBD 2021 study. Front Nutr. 2025;12:1652676.

[29] Qiu X, Hu B, Ke J, Wang M, Zeng H, Gu J. Global, regional, and national trends in peripheral arterial disease among older adults: findings from the Global Burden of Disease Study 2021. Aging Clin Exp Res. 2025;37(1):150.

[30] Qu J, Zeng Z, Huo W, He M, Bao X, Lu Y, et al. Global burden of lower extremity peripheral arterial disease associated with high fasting plasma glucose: an analysis of the Global Burden of Disease Study 2021. Eur J Vasc Endovasc Surg. 2025.

[31] Zhang G, Liu X, Li J, Zhao Y, Yuan Z, Chen Y, et al. Global, regional, and national burdens of lower extremity peripheral arterial disease from 1990 to 2021 and projections to 2050: Global Burden of Disease Study 2021. Front Cardiovasc Med. 2025;12:1592322.

[32] Fu M, Zhang H. Global burden of peripheral arterial disease and its risk factors, 1990–2021. BMC Cardiovasc Disord. 2025;25:631.

[33] Wang MS, Deng JW, Geng WY, Zheng R, Xu HL, Dong Y, et al. Temporal trend and attributable risk factors of cardiovascular disease burden for adults 55 years and older in 204 countries/territories from 1990 to 2021: an analysis for the Global Burden of Disease Study 2021. Eur J Prev Cardiol. 2025;32(7):539–52.

[34] Cheng X, Yang Y, Schwebel DC, Liu Z, Li L, Cheng P, et al. Population ageing and mortality during 1990–2017: a global decomposition analysis. PLoS Med. 2020;17(6):e1003138.

[35] Joynt Maddox KE, Elkind MSV, Aparicio HJ, Commodore-Mensah Y, de Ferranti SD, Dowd WN, et al. Forecasting the burden of cardiovascular disease and stroke in the United States through 2050—prevalence of risk factors and disease: a presidential advisory from the American Heart Association. Circulation. 2024;150(4):e65–88.

[36] GBD 2021 Causes of Death Collaborators. Global burden of 288 causes of death and life expectancy decomposition in 204 countries and territories and 811 subnational locations, 1990–2021: a systematic analysis for the Global Burden of Disease Study 2021. Lancet. 2024;403(10440):2100–32.

[37] Institute for Health Metrics and Evaluation (IHME). GBD Results Tool. Seattle, WA: IHME, University of Washington; 2025. GBD Results Tool. Accessed [insert date].

[38] Stevens GA, Alkema L, Black RE, Boerma JT, Collins GS, Ezzati M, et al. Guidelines for Accurate and Transparent Health Estimates Reporting: the GATHER statement. Lancet. 2016;388(10062):e19–23.

[39] GBD 2019 Risk Factors Collaborators. Global burden of 87 risk factors in 204 countries and territories, 1990–2019: a systematic analysis for the Global Burden of Disease Study 2019. Lancet. 2020;396(10258):1223–49.

[40] Metcalf PA, Scragg RKR. Comparison of WHO and ADA criteria for diagnosis of glucose status in adults. Diabetes Res Clin Pract. 2000;49(2–3):169–80.

[41] GBD 2019 Diseases and Injuries Collaborators. Global burden of 369 diseases and injuries in 204 countries and territories, 1990–2019: a systematic analysis for the Global Burden of Disease Study 2019. Lancet. 2020;396(10258):1204–22.

[42] Hankey BF, Ries LA, Kosary CL, Feuer EJ, Merrill RM, Clegg LX, et al. Partitioning linear trends in age-adjusted rates. Cancer Causes Control. 2000;11(1):31–5.

[43] Das Gupta P. Standardization and decomposition of rates: a user's manual. Current Population Reports, Series P23-186. Washington, DC: US Bureau of the Census; 1993.

[44] Hyndman RJ, Athanasopoulos G. Forecasting: principles and practice. 3rd ed. Melbourne: OTexts; 2021.

[45] Hyndman RJ, Khandakar Y. Automatic time series forecasting: the forecast package for R. J Stat Softw. 2008;27(3):1–22.

[46] Chen T, Guestrin C. XGBoost: a scalable tree boosting system. In: Proceedings of the 22nd ACM SIGKDD International Conference on Knowledge Discovery and Data Mining. New York: ACM; 2016. p. 785–94.

[47] Hochreiter S, Schmidhuber J. Long short-term memory. Neural Comput. 1997;9(8):1735–80.

[48] Oreshkin BN, Carpov D, Chapados N, Bengio Y. N-BEATS: neural basis expansion analysis for interpretable time series forecasting. In: International Conference on Learning Representations (ICLR); 2020. arXiv:1905.10437.

[49] Foreman KJ, Marquez N, Dolgert A, Fukutaki K, Fullman N, McGaughey M, et al. Forecasting life expectancy, years of life lost, and all-cause and cause-specific mortality for 250 causes of death: reference and alternative scenarios for 2016–40 for 195 countries and territories. Lancet. 2018;392(10159):2052–90.

[50] Komosinska-Vassev K, Olczyk K, Olczyk P, Winsz-Szczotka K. Effects of metabolic control and vascular complications on indices of oxidative stress in type 2 diabetic patients. Diabetes Res Clin Pract. 2005;68(3):207–16.

[51] Ogurtsova K, Guariguata L, Barengo NC, Ruiz PL, Sacre JW, Karuranga S, et al. IDF Diabetes Atlas: global estimates of undiagnosed diabetes in adults for 2021. Diabetes Res Clin Pract. 2022;183:109118.

[52] Gornik HL, Aronow HD, Goodney PP, Arya S, Brewster LP, Byrd L, et al. 2024 ACC/AHA/AACVPR/APMA/ABC/SCAI/SVM/SVN/SVS/SIR/VESS guideline for the management of lower extremity peripheral artery disease: a report of the American College of Cardiology/American Heart Association Joint Committee on Clinical Practice Guidelines. Circulation. 2024;149(24):e1313–410.

[53] American Diabetes Association Professional Practice Committee. 10. Cardiovascular disease and risk management: Standards of Care in Diabetes—2024. Diabetes Care. 2024;47(Suppl 1):S179–218.

[54] Haile KE, Asgedom YS, Azeze GA, Amsalu AA, Kassie GA, Gebrekidan AY. Burden of peripheral artery disease and risk factors among patients with diabetes mellitus in sub-Saharan Africa: a systematic review and meta-analysis. BMC Endocr Disord. 2025;25(1):42.